Biomaterials Science

ROYAL SOCIETY OF CHEMISTRY

PAPER

View Article Online
View Journal | View Issue

Cite this: *Biomater. Sci.*, 2024, **12**, 3112

Photocrosslinkable microgels derived from human platelet lysates: injectable biomaterials for cardiac cell culture

Sara C. Santos, Catarina A. Custódio * and João F. Mano *

Received 27th November 2023,
Accepted 23rd April 2024

DOI: 10.1039/d3bm01933k

rsc.li/biomaterials-science

Cardiovascular diseases are a major global cause of morbidity and mortality, and they are often characterized by cardiomyocytes dead that ultimately leads to myocardial ischemia (MI). This condition replaces functional cardiac tissue with fibrotic scar tissue compromising heart function. Injectable systems for the *in situ* delivery of cells or molecules to assist during tissue repair have emerged as promising approaches for tissue engineering, particularly for myocardial repair. Methacryloyl platelet lysates (PLMA) have been employed for constructing full human-based 3D cell culture matrices and demonstrated potential for xeno-free applications. In this study, we propose using PLMA to produce microparticles (MPs) serving as anchors for cardiac and endothelial cells and ultimately as injectable systems for cardiac tissue repair. The herein reported PLMA MPs were produced by droplet microfluidics and showed great properties for cell attachment. More importantly, it is possible to show the capacity of PLMA MPs to serve as cell microcarriers even in the absence of animal-derived serum supplementation in the culture media.

1. Introduction

Cardiovascular diseases are a major cause of morbidity and mortality worldwide. Myocardial ischemia (MI) is characterized by death of cardiomyocytes commonly caused by prolonged ischemia and myocardial perfusion reduction after the occlusion of a coronary artery. This results in the replacement of functional myocardial tissue with fibrotic scar tissue and ventricular remodelling, leading to malfunction of the heart.[1–3] Current treatments for myocardial repair include pharmacological and surgical techniques to restore blood supply to the infarcted area; however, such approaches are not able to reverse the condition. As such, cell-based therapies and local delivery of molecules such as growth factors (GFs) have emerged to enhance infarcted myocardium tissue regeneration.[4] However, the rapid wash of injected cells and the hostility of the infarcted myocardium environment are problems related with these therapies.[1] Therefore, biomaterials have been emerging as possible solutions to overcome such issues.[5]

Microcarriers have emerged as potential delivery platforms for cell-based tissue engineering strategies as they offer the possibility to optimize cell engraftment and survival upon transplantation.[6] In this context, an effort on the development of biocompatible microparticles (MPs) has been made over the past decades. These innovative MPs serve as effective cell carriers and can be seamlessly integrated into minimally invasive, injectable systems for *in situ* cell delivery.[7–9] In particular, in the field of cardiac tissue regeneration, MPs have been explored not only as vehicles to deliver cells *in situ*[10–13] but also as carriers of cells and/or therapeutic agents[14–19] for myocardial tissue repair. Besides this, applications of MPs to fabricate granular injectable hydrogels for *in situ* cardiac tissue repair have also been reported.[20,21]

Human platelet lysates (hPL) have been explored for multiple applications as an autologous source of GFs and bioactive proteins that play roles in cell adhesion, proliferation, and growth.[22,23] Regarding tissue engineering approaches, hPL have been studied as a material to produce biocompatible matrices; however, these platforms usually suffer from poor mechanical properties and stability *in vitro*. As such, methacryloyl platelet lysates (PLMA) have been recently reported as a precursor to produce scaffolds for 3D cell culture.[24] These innovative scaffolds offer enhanced stability and flexibility with finely tuned mechanical control, effectively overcoming the limitations associated with conventional hPL-based matrices. The synthesized hydrogels have been proven to support growth, sprouting and migration of human-derived cells,[24,25] as well as having great potential to be used as platforms to study tumor invasion behavior of cancer cells.[26,27] Moreover, it was also reported that PLMA-based porous scaffolds are capable of supporting cell maintenance and function in the absence of animal-derived serum supplements.[28]

As such, in this work, we explore the potential of PLMA as a precursor material to produce MPs to be used as cell carriers

Department of Chemistry, CICECO – Aveiro Institute of Materials, University of Aveiro, Portugal. E-mail: catarinacustodio@ua.pt, jmano@ua.pt

in xeno-free conditions and ultimately serve as injectable systems for tissue repair. PLMA-based MPs were produced by droplet microfluidics and their ability to anchor cardiac and endothelial cells was evaluated. Due to their richness in GFs and bioactive proteins, our hypothesis is that PLMA-based MPs will be able to support the culture of cardiac and endothelial cells even in the absence of animal-derived serum supplements commonly used in cell culture. Notably, these MPs can be used in an autologous form, derived from the patient's own blood, presenting a valuable option for creating tailor-made, robust matrices. This approach eliminates concerns regarding cross-reactivity, immune responses, or disease transmission, making it a versatile and safe choice for tissue-engineering applications.

2. Materials and methods

2.1. Methacryloyl platelet lysates (PLMA) synthesis

PLMA was synthesized following a previously reported protocol.[24] Briefly, human platelet lysates (hPL, STEMCELL Technologies, Canada) were reacted with methacrylic anhydride 94% (MA) (Sigma-Aldrich, Germany) under constant stirring at room temperature. The synthesized PLMA was then purified by dialysis against deionized water to remove the excess of MA. The PLMA solution was afterwards freeze-dried and stored at +4 °C until further use.

2.2. PLMA and gelatin methacryloyl (GelMA) microparticles (MPs) production by droplet microfluidics

PLMA was dissolved in phosphate-buffered saline (PBS, Sigma-Aldrich) with 0.5% (w/v) 2-hydroxy-4′-(2-hydroxyethoxy)-2-methylpropiophenone (Irgacure 2959, Sigma-Aldrich) to a final concentration of 15% (w/v) PLMA. PLMA MPs were produced by droplet generation using a hydrophobic droplet junction chip with header (190 μm etch depth) (Dolomite, UK). Water-in-oil microdroplets were produced by using PLMA 15% (w/v) as a dispersed phase and mineral oil (pure, Thermo Scientific, USA) as a continuous phase. Flow rates for both dispersed and continuous phases were controlled by a programmable dual-drive syringe pump (Pump 33 DDS, Harvard Apparatus, USA). PLMA microdroplets were afterwards photocrosslinked by exposure to ultraviolet (UV) irradiation (0.2 W cm^{-2}, OmniCure S2000 Spot UV Curing System, Excelitas Technologies Corp., USA) for 30 seconds. PLMA MPs were then washed with 0.1% (v/v) Triton™ X-100 BioXtra (Sigma-Aldrich) solution in PBS to remove the oil. Washing steps were performed for 10 minutes in a water bath at 37 °C with agitation (100 rpm) until complete elimination of the oil. Following the same procedure, GelMA MPs were produced and used as a control in this work. Gelatin methacryloyl (300 g Bloom, 80% degree of substitution, Merck, Germany) was dissolved in PBS with 0.5% Irgacure 2959 to a final concentration of 10% (w/v) GelMA and used as a dispersed phase. Flow rates for GelMA microdroplets production were set to be the same as those used for PLMA and photocrosslinking was also performed afterwards. GelMA MPs were then washed with 0.1% (v/v) Triton™ X-100 BioXtra in PBS to remove the oil. The morphology of PLMA and GelMA MPs was assessed by optical microscopy (Primovert microscope stand with binocular phototube, Zeiss, Germany) and images were analysed by ImageJ software for size measurements of MPs.

2.3. MPs characterization by scanning electron microscopy (SEM)

PLMA and GelMA MPs were produced as described in section 2.2. The SEM examination was performed using an SEM Hitachi SU-3800 (Hitachi, Japan) instrument coupled to a Standard SEM Coolstage at −25 °C to +50 °C (Deben, UK). After the production of PLMA and GelMA MPs as described in section 2.2, the specimens were transferred in their hydrated state into an SEM chamber and cooled to be studied at −25 °C under vacuum.

2.4. PLMA MPs protein release assays and quantification

For protein release assays, PLMA MPs were immersed in 5 mL of PBS and incubated in a water bath at 37 °C with constant agitation (100 rpm). At pre-determined time points, an aliquot of 1 mL volume was taken from each sample and replaced with fresh PBS. Collected samples were stored at −20 °C until further use. Total protein quantification was performed with a Micro BCA protein assay kit (Thermo Fisher Scientific). Quantification of specific GFs was also performed by using a LEGENDplex™ Human Growth Factor Panel (13-plex) (Biolegend, USA) according to the manufacturer's instructions. The LEGENDPLEX™ assay is based on the conjugation of specific antibodies, and is therefore a very specific recognition method for molecules of interest. This kit is a bead-based multiplex assay that allows the quantification of 13 different GFs simultaneously: angiopoietin-2, epidermal growth factor (EGF), erythropoietin (EPO), basic fibroblast growth factor (FGF-basic), granulocyte colony-stimulating factor (G-CSF), granulocyte-macrophage colony-stimulating factor (GM-SCF), hepatocyte growth factor (HGF), macrophage colony-stimulating factor (M-CSF), platelet-derived growth factor AA (PDGF-AA), platelet-derived growth factor BB (PDGF-BB), stem cell factor (SCF), transforming growth factor alpha (TGF-α), and vascular endothelial growth factor (VEGF). Quantification of specific GFs in both hPL and PLMA was also performed. Total protein and LEGENDPlex™ values were expressed as mean ± standard deviation ($n \geq 3$).

2.5. MPs *in vitro* cell culture

MPs' ability to anchor cardiac and endothelial cells was evaluated using the H9c2(2-1) cell line from rat BDIX heart myoblasts (Sigma-Aldrich) and human umbilical vein endothelial cells (HUVECs). H9c2(2-1) cells were cultured in Dulbecco's modified Eagle's medium high glucose (DMEM HG, Sigma-Aldrich), supplemented with 10% FBS (v/v) (Thermo Fisher Scientific) and 1% (v/v) antibiotic/antimycotic (Thermo Fisher Scientific). These cells were used between passages 13 and 27 and cultured in a humidified incubator with a 5% CO_2 atmo-

sphere at 37 °C. HUVECs were isolated from umbilical cord obtained under a cooperation agreement between the University of Aveiro and Centro Hospitalar do Baixo Vouga (CHBV, Aveiro, Portugal), approved by the Ethics Commission. Informed consent was obtained from all subjects. The sample was transported in PBS supplemented with 1% (v/v) antibiotic/antimycotic and stored at +4 °C until isolation. Umbilical cord was washed with PBS and a 0.1% (w/v) type I collagenase (MP Biomedicals, USA) was injected within the umbilical cord vein. After 45 minutes of incubation at 37 °C, the umbilical vein was injected with Medium 199 (M199, Sigma-Aldrich) supplemented with 20% (v/v) FBS, 1% (v/v) antibiotic/antimycotic, 1% (v/v) GlutaMAX™ supplement (Thermo Fisher Scientific), 0.1% (v/v) heparin (100 mg mL^{-1}, PanReac AppliChem, Spain) and 0.01% (v/v) endothelial cell growth supplement (ECGS, Sigma-Aldrich) to collect the cells. The cell suspension was afterwards transferred to a cell culture flask. Cells were cultured in a humidified incubator with a 5% CO_2 atmosphere at 37 °C. The culture medium was changed after 24 hours and then every 2–3 days.

For cell culture assays, PLMA and GelMA MPs were obtained following the procedure described in section 2.2. Afterwards, MPs were incubated in a 1% (v/v) antibiotic/antimycotic solution in PBS for 2 hours in a 37 °C water bath with agitation (100 rpm). MPs were then transferred to a microplate well and the cell suspension was afterwards dispensed in the well along with the MPs. Monoculture of H9c2(2-1) cells and co-culture assays using H9c2(2-1) cells and HUVECs were performed. For the monoculture assay, H9c2(2-1) cells were seeded in a ratio of 150 cells per microparticle. Cells were cultured for 7 days in DMEM HG with or without FBS supplementation. In the co-culture assay, a total ratio of 150 cells per microparticle was maintained, with a 7 : 3 ratio of cardiac to endothelial cells. Cells were cultured for 7 days in a mixture of DMEM HG and M199, with the option of FBS supplementation.

Live/dead fluorescence assay. At pre-determined time-points (3 and 7 days of cell culture), live/dead assay was performed. PLMA and GelMA MPs with cells were incubated in a solution of 2 μL of 4 mM Calcein AM in DMSO (Thermo Fisher Scientific) and 1 μL of 1 mg mL^{-1} propidium iodide (PI, Thermo Fisher Scientific) in 1 mL of PBS for 30 minutes at 37 °C. After washing with PBS, MPs were examined using a fluorescence microscope (Axio Imager 2, Zeiss, Germany). Image processing was performed using ZEN v3.1 blue edition software (Carl Zeiss Microscopy GmbH).

DAPI/phalloidin staining. For cell morphology assessment, DAPI/phalloidin staining was performed. At pre-determined time-points, PLMA MPs were washed with PBS and fixed with a 4% (v/v) paraformaldehyde (PFA, Sigma-Aldrich) solution in PBS. A phalloidin solution (Flash Phalloidin™ Red 594, 300U, Biolegend) 1 : 40 in PBS was prepared and MPs were incubated at room temperature for 30 minutes. After washing with PBS, a 4′,6-diamidino-2-phenylindole dihydrochloride (DAPI, Thermo Fisher Scientific) solution was diluted 1 : 1000 in PBS and the MPs were incubated for 5 minutes at room temperature. Subsequently, the MPs were examined using a confocal microscope (LSM 900, Zeiss). Image processing was performed using ZEN v3.4 blue edition software (Carl Zeiss Microscopy GmbH).

Cardiac troponin T (cTnT) and CD31 immunostaining. After 7 days of cell culture, PLMA MPs were washed with PBS and fixed in a 4% (v/v) PFA solution in PBS. Following fixation, the samples were permeabilized with 0.1% (v/v) Triton™ X-100 BioXtra in PBS for 15 minutes. After washing with PBS, PLMA MPs were blocked with 5% (v/v) FBS in PBS for 45 minutes. For staining H9c2(2-1) cells, anti-troponin T-C antibody (CT3) (Santa Cruz Biotechnology, USA) was diluted 1 : 100 in 5% (v/v) FBS/PBS and incubated overnight at +4 °C. After washing with PBS, the samples were incubated for 2 hours at room temperature with anti-mouse Alexa Fluor 488 (Thermo Fisher Scientific) 1 : 500 in 5% (v/v) FBS/PBS. For staining HUVECs, anti-human CD31 antibody (Biolegend) was diluted 1 : 200 in 5% (v/v) FBS/PBS and incubated overnight at +4 °C. After washing with PBS, the samples were incubated for 2 hours at room temperature with anti-mouse Alexa Fluor 647 (Thermo Fisher Scientific) 1 : 200 in 5% (v/v) FBS/PBS. After washing, a DAPI solution was diluted 1 : 1000 in PBS and MPs were incubated for 5 minutes at room temperature. Afterwards, the samples were examined using a confocal microscope (LSM 900, Zeiss). Image processing was performed using ZEN v3.4 blue edition software (Carl Zeiss Microscopy GmbH).

Cell counting kit-8 (CCK-8). Cell counting kit-8 (CCK-8, MedChemExpress, USA) was used to evaluate the cell viability. At pre-determined time-points, samples were incubated in a solution of CCK-8 reagent diluted in medium following the manufacturer's instructions. Samples were then incubated for 4 hours at 37 °C, protected from light. The quantification was achieved by measuring absorbance at 450 nm (Microplate reader – SpectraMax iD3 Multi-Mode, Molecular Devices, USA). Triplicates of each sample were made per culturing time. CCK-8 values were expressed as mean ± standard deviation (n = 6).

DNA quantification. Total DNA quantification was performed after cell lysis using a Quant-iT PicoGreen dsDNA kit (Thermo Fisher Scientific). At pre-determined time-points, MPs were washed with PBS, incubated in sterile deionized water and frozen at −80 °C. In order to induce disruption of the cells, freeze (−80 °C) and thaw (37 °C) cycles were performed. Samples were processed according to the specifications of the kit and DNA standards were prepared with concentrations ranging from 0 to 2 μg mL^{-1} from the dsDNA solution provided in the kit. After 10 minutes of incubation in the dark at room temperature, fluorescence was measured using an excitation wavelength of 480 nm and an emission wavelength of 528 nm (Microplate reader – SpectraMax iD3 Multi-Mode, Molecular Devices). Triplicates of each sample were made per culturing time. DNA values were expressed as mean ± standard deviation (n = 6).

2.6. Statistical analysis

All data were subjected to statistical analysis and values were reported as mean ± standard deviation. Statistical differences between the analysed groups were determined by one-way

ANOVA or two-way ANOVA with Tukey's multiple comparisons test where $p < 0.05$ values were considered statistically significant. All statistical analyses were performed using GraphPad Prism 8 software.

3. Results and discussion

3.1. Characterization of PLMA MPs

PLMA is a photocrosslinkable material composed of several bioactive proteins and GFs obtained by the reaction of human platelet lysates (hPL) with MA. ^{1}H-NMR and mass spectrometry analyses carried out in a previous work showed successful functionalization of hPL with methacryloyl groups, as well as the observation that the most abundant and, therefore, the most modified protein in the mixture is human serum albumin.[24] In this work, PLMA MPs were produced by droplet microfluidics using a hydrophobic droplet junction chip. After droplet formation within the microfluidic chip channels, PLMA droplets were photocrosslinked to produce PLMA MPs. Fig. 1A shows a schematic representation of the process and Fig. 1B the microfluidics setup for the production of MPs. Droplet microfluidics allows the generation of microdroplets with precise control of the size of the resulting MPs.[29] As a result, the PLMA MPs generated in this study exhibit a uniformly round shape, as illustrated in Fig. 1C. Moreover, it was possible to produce MPs with different sizes by changing the PLMA solution flow rate during formation of microdroplets. Lower flow rates allow the production of smaller MPs with a size of about 195 μm (Fig. 1C.1). When increased flow rates were used, MPs with larger sizes were produced, as shown by the results of size distribution graphs (Fig. 1C.2 and 1C.3), where it is possible to form MPs with sizes of around 270 μm or 320 μm. Apart from the production of MPs with a uniformly round shape, we can observe that for lower (Fig. 1C.1) or higher flow rates (Fig. 1C.3), the frequency of the size distribution for PLMA MPs does not fit the bell-shaped curve as well as that for the MPs produced with the intermediate flow rate (Fig. 1C.2). In that case, PLMA MPs demonstrate a narrow size distribution spanning from 240 μm to 300 μm and therefore these PLMA MPs were chosen for use in this work. In order to assess the morphology and topographical features of PLMA MPs, SEM analysis at −25 °C was performed. Fig. 1E is a representative image of PLMA MPs showing their round shape as well as their porous surface. As previously mentioned, GelMA MPs were also produced using the same technique and were used as a control for cell culture assays. GelMA MPs also showed a round shape (Fig. 1D) and narrow size distribution ranging from 240 μm until 300 μm (Fig. 1D). Moreover, SEM analysis at −25 °C showed that GelMA MPs have a porous surface as well (Fig. 1F).

3.2. Protein release of PLMA MPs

hPL are a pool of bioactive proteins and GFs essential for cell maintenance and growth. As a result, extensive research has been conducted to substitute the commonly used animal-derived serum supplements in cell culture for hPL, enhancing clinical relevance and minimizing the risk of contamination. Although the composition of GFs in FBS and hPL is very similar, hPL presents an increased concentration of GFs when compared to FBS. For example, quantification of GFs like platelet-derived growth factors (PDGFs), basic fibroblast growth factor (FGF-basic), epidermal growth factor (EGF), vascular endothelial growth factor (VEGF), transforming growth factor-β1 (TGF-β1) or insulin-like growth factor-1 (IGF-1) showed significant differences in content between FBS and hPL, with much higher quantities being found in hPL formulations.[30] As such, hPL shows great potential to be a better alternative for cell culture in xeno-free conditions, thus avoiding issues related to cross-reactivity, immune reaction or disease transmission due to the presence of animal-derived components.[31] The quantification of GFs in both hPL and PLMA was assessed using the LEGENDplex™ Human Growth Factor Panel – see Fig. 2A and B. Results show that hPL and PLMA are rich in GFs known to be involved in cell maintenance and therefore have the potential to be used as sources to engineer systems for xeno-free cell culture.

In a previous work, PLMA was indeed reported as a precursor material to produce porous matrices to culture human stem cells in the absence of animal-derived serum supplements. Such scaffolds were able to support adhesion, proliferation and growth of human adipose stem cells (hASCs) for 14 days when cultured in xeno-free conditions.[28] Taking this into consideration, herein we hypothesized that the GFs and bioactive proteins present in PLMA could be gradually released from PLMA MPs, being helpers in the attachment and maintenance of cardiac and endothelial cells. In this sense, protein release assays of PLMA MPs were performed to quantify bioactive proteins and GFs that can be involved in cell maintenance during cell culture assays in xeno-free conditions. Fig. 2C shows an overall sustained release of proteins from PLMA MPs for 14 days. These results can corroborate our hypothesis that PLMA MPs are able to release proteins that can maintain cell viability during the culture time. In addition, quantification of specific GFs in the supernatants collected during protein release assays was assessed using the same procedure to quantify GFs in hPL and PLMA. The results for the quantification of these GFs are presented in Fig. 2D, and we can also observe a controlled release of these proteins over time. The GFs here identified are known to be key helpers in cell proliferation and maintenance. PDGFs, for instance, are inducers of cellular processes that ultimately lead to matrix modulation and, as a consequence, tissue repair.[32] Along with VEGF, PDGFs play a pivotal role in the angiogenesis process – a mandatory step during tissue repair – and therefore are both important molecules when it comes to tissue repair after MI, for example.[32,33] Other GFs released by PLMA MPs, like FGF, have also been proven to be involved in tissue repair processes, stimulating cell proliferation and migration during tissue healing.[34]

These results support our hypothesis that PLMA MPs can release bioactive proteins and GFs over time, thereby contributing to cell maintenance and survival. The abundance of

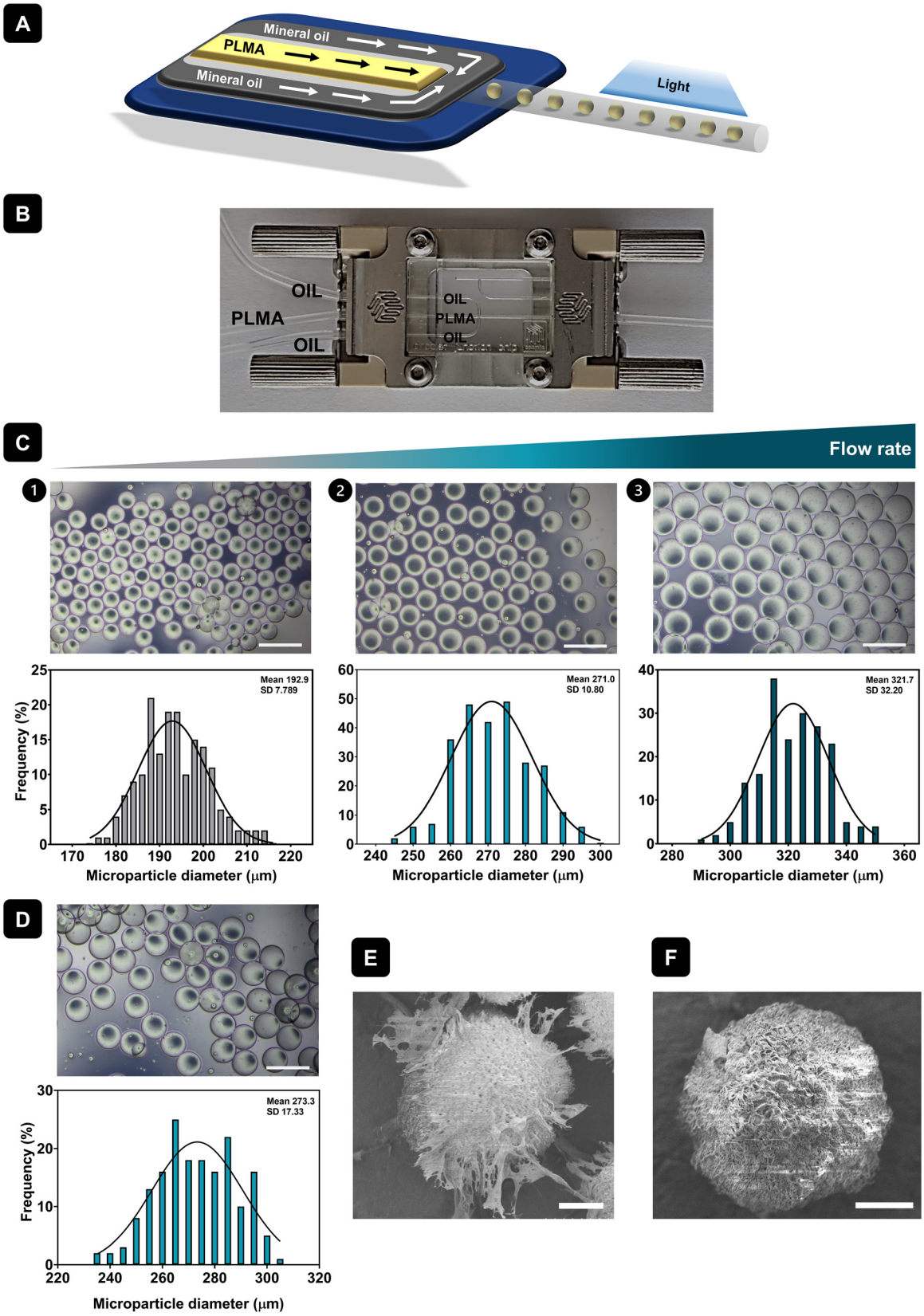

Fig. 1 Production and characterization of PLMA MPs. (A) Schematic representation of the production of MPs by droplet microfluidics. (B) Microfluidics setup for production of MPs. (C) Representative optical microscope images and size distribution graphs of PLMA MPs produced with different flow rates. Scale bar: 500 μm. (D) Representative optical microscope image and size distribution graph of GelMA MPs. Scale bar: 500 μm. Representative SEM image of (E) PLMA and (F) GelMA MPs. Scale bar: 50 μm.

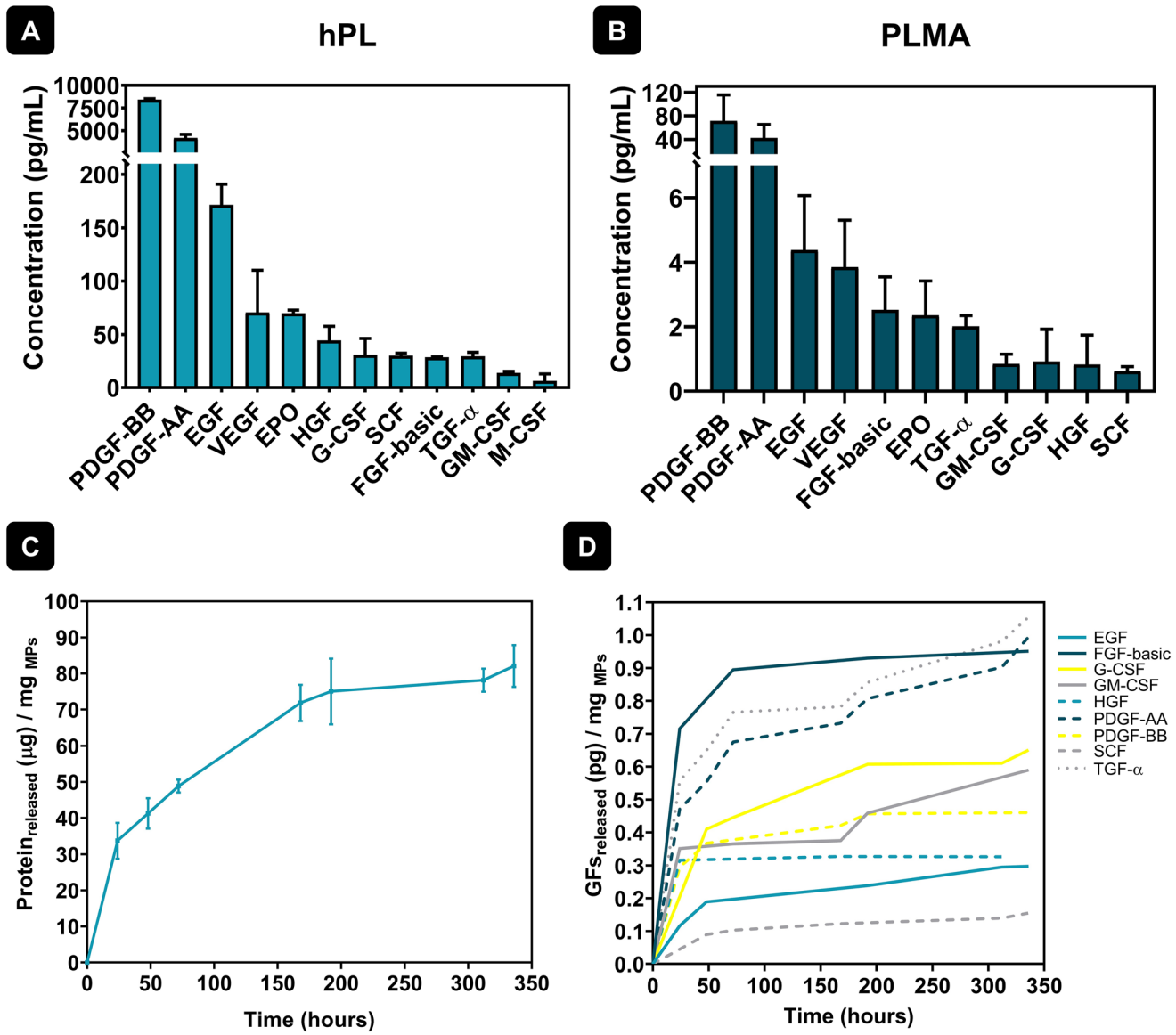

Fig. 2 Quantification of hPL and PLMA GFs and the protein release profile of PLMA MPs. Quantification of hPL (A) and PLMA (B) GFs using the LEGENDplex™ Human Growth Factor Panel. (C) Cumulative protein release from PLMA MPs over 14 days. (D) Cumulative release of GFs from PLMA MPs over 14 days.

these molecules in hPL and PLMA is a crucial factor in the development of platforms and systems for cell culture and tissue repair that eliminate the need for commonly used animal-derived serum supplements, which can often be a barrier during clinical translation.

3.3. *In vitro* cell culture in PLMA and GelMA MPs

In recent years, there has been a significant effort to replace animal-derived serum supplements in the development of cell culture platforms. One major reason for this shift is the risk of disease and xenogeneic contamination associated with animal-derived serum supplements, as well as ethical concerns about serum collection methods. Consequently, materials based on hPL are attractive options for the development of 3D cell culture platforms and systems to promote tissue repair upon implantation.[22] As such, herein PLMA MPs were explored for the development of injectable systems for cardiac and endothelial cell culture and ultimately for tissue repair.

H9c2(2-1) cells were cultured in PLMA MPs (monoculture, MONO) using both media with and without animal-derived serum supplementation. Besides this, and due to the importance of neovascularization during tissue repair, the co-culture (CO) of H9c2(2-1) cells with endothelial cells (HUVECs) was also explored using PLMA MPs as cell carriers (Fig. 3A). Co-culture assays were also performed in media with and without FBS supplementation.

To assess cell viability during culture time, live/dead staining was performed at 3, 7 and 14 days of culture. As shown in

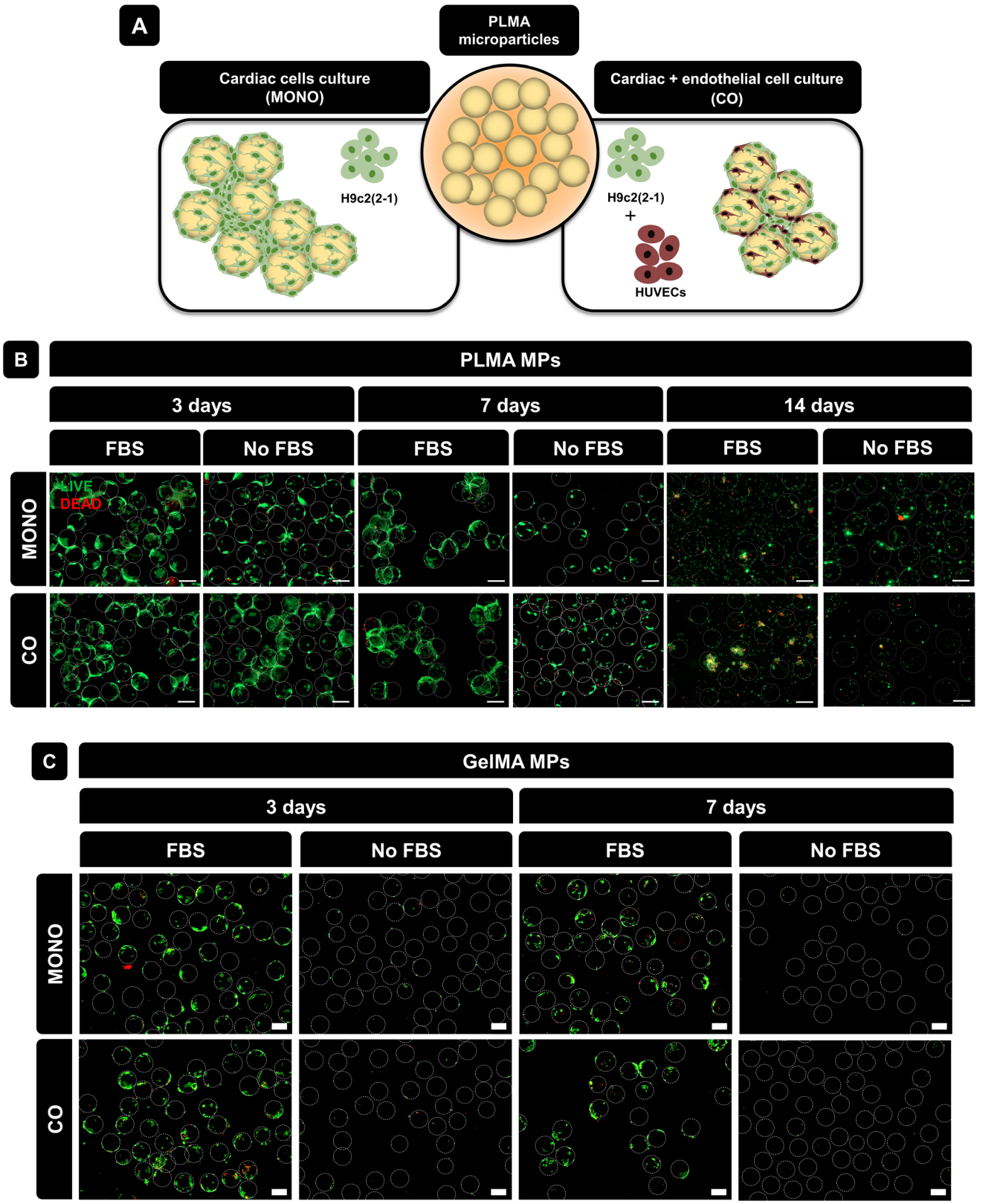

Fig. 3 Live/dead assay. (A) Representative scheme of cell culture studies. (B) Representative live/dead images of H9c2(2-1) (MONO) and H9c2-(2-1) + HUVECs (CO) cultured with PLMA MPs at 3, 7 and 14 days of culture with and without FBS. (C) Representative live/dead images of H9c2(2-1) (MONO) and H9c2-(2-1) + HUVECs (CO) cultured with GelMA MPs at 3 and 7 days of culture with and without FBS. Scale bar: 200 μm.

Fig. 3B, for both monoculture and co-culture conditions, cells were able to adhere to PLMA MPs and form aggregates at 3 days of culture. Even in the absence of animal-derived serum supplementation, cells could adhere to the MPs and survive for up to 7 days. Nevertheless, it is possible to observe a decrease in the cell–MPs interaction for longer cell culture times, especially in no-serum conditions, which can be explained by the fact that there is no serum replacement over time and therefore an insufficient amount of GFs is supplied by PLMA MPs for cell maintenance. It is also possible to observe that increasing the cell culture time (14 days) does not benefit the cell–MPs interaction even when FBS is present in the media, which can be explained by the higher cell proliferation rate in comparison with the available surface area for cell adhesion. GelMA MPs were used for comparison since they do not release GFs and are generally not expected to support cell culture without serum. Fig. 3C shows the live/dead images of cells cultured in GelMA MPs under the same conditions as those for PLMA MPs and it can be observed that although cells were able to adhere and remain viable in the presence of FBS, in the absence of animal-derived serum supplementation, cells were not able to adhere to GelMA MPs due to the lack of bioactive proteins to promote cell maintenance.

Cell viability by CCK-8 testing was also measured and results showed maintenance of cell viability from 3 to 7 days of culture when cells were cultured with PLMA MPs – see Fig. 4A. Moreover, it can also be observed that co-culture of cardiac and endothelial cells increases the cell viability in the system and therefore the addition of endothelial cells promotes cell adhesion to the MPs and maintenance over time. In contrast, when GelMA MPs were used as cell microcarriers, the cell viability decreased from day 3 to day 7 in the conditions where FBS was present in the media. Moreover, and as expected, when cultured in the absence of animal serum supplementation, the cells were unable to adhere and maintain viability, as demonstrated by the substantial difference in cell viability between the conditions with FBS and those without supplementation – see Fig. 4A. DNA quantification was also performed to assess the proliferation of cells cultured in both PLMA MPs and GelMA MPs, providing additional support for the observed trends. DNA quantification supported these findings, showing sustained levels in cells cultured with PLMA MPs compared to GelMA MPs, where a decrease in DNA content was evident, especially under conditions without medium supplementation.

Morphological features of cells cultured in PLMA MPs were assessed by staining the F-actin filaments (phalloidin, red) and nuclei (DAPI, blue). Fig. 5A shows that the cells were spread around PLMA MPs, and small aggregates of cells and MPs were formed only at 3 days of culture under all conditions of the analysis. Besides that, and in order to assess the expression of specific markers of both cardiac and endothelial cells, immunostaining with specific antibodies was performed: cardiac troponin T (cTnT) for H9c2(2-1) and CD31 for HUVECs. Confocal images presented in Fig. 5B show the expression of these specific markers in both cell types under

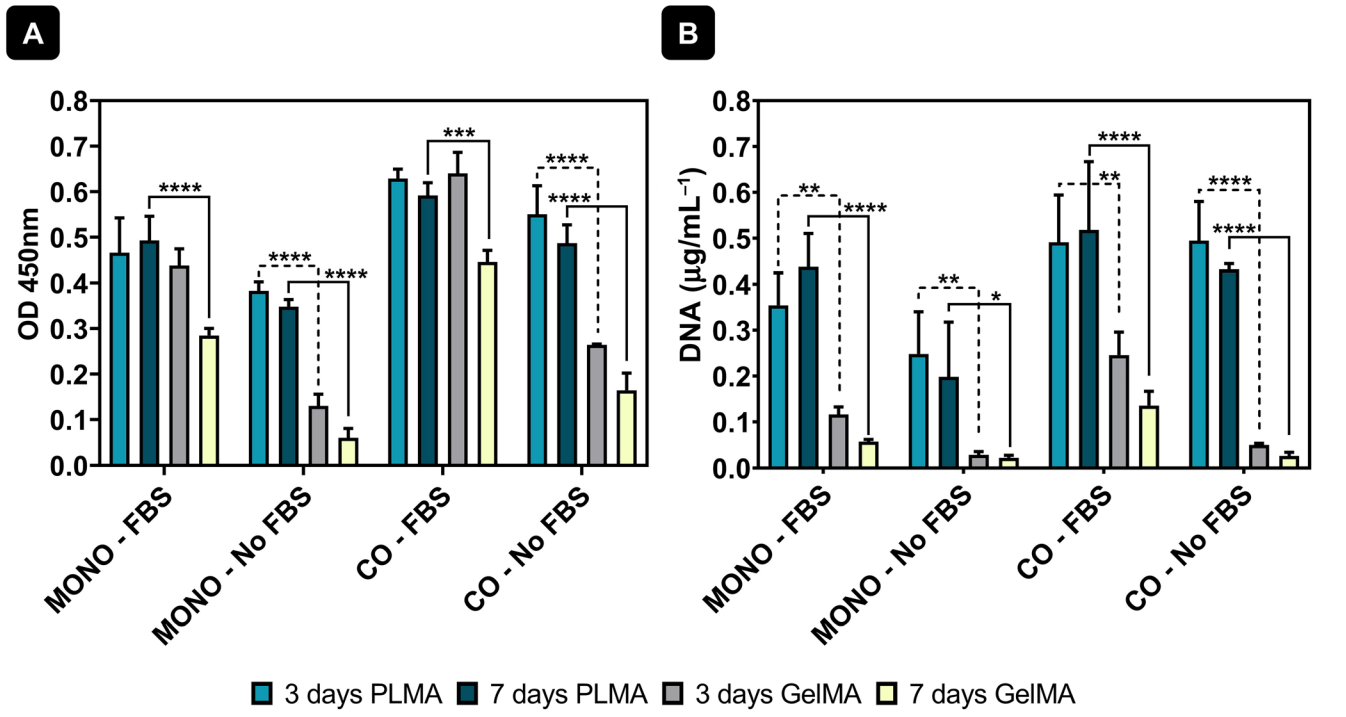

Fig. 4 Cell viability and cell proliferation. (A) CCK-8 test results and (B) DNA quantification results for cells cultured in PLMA MPs and GelMA MPs at 3 and 7 days of culture. Statistical analysis through two-way ANOVA combined with Tukey's multiple comparisons test showed significant differences between the analysed groups: *$p < 0.05$, **$p < 0.01$, ***$p < 0.001$, and ****$p < 0.0001$.

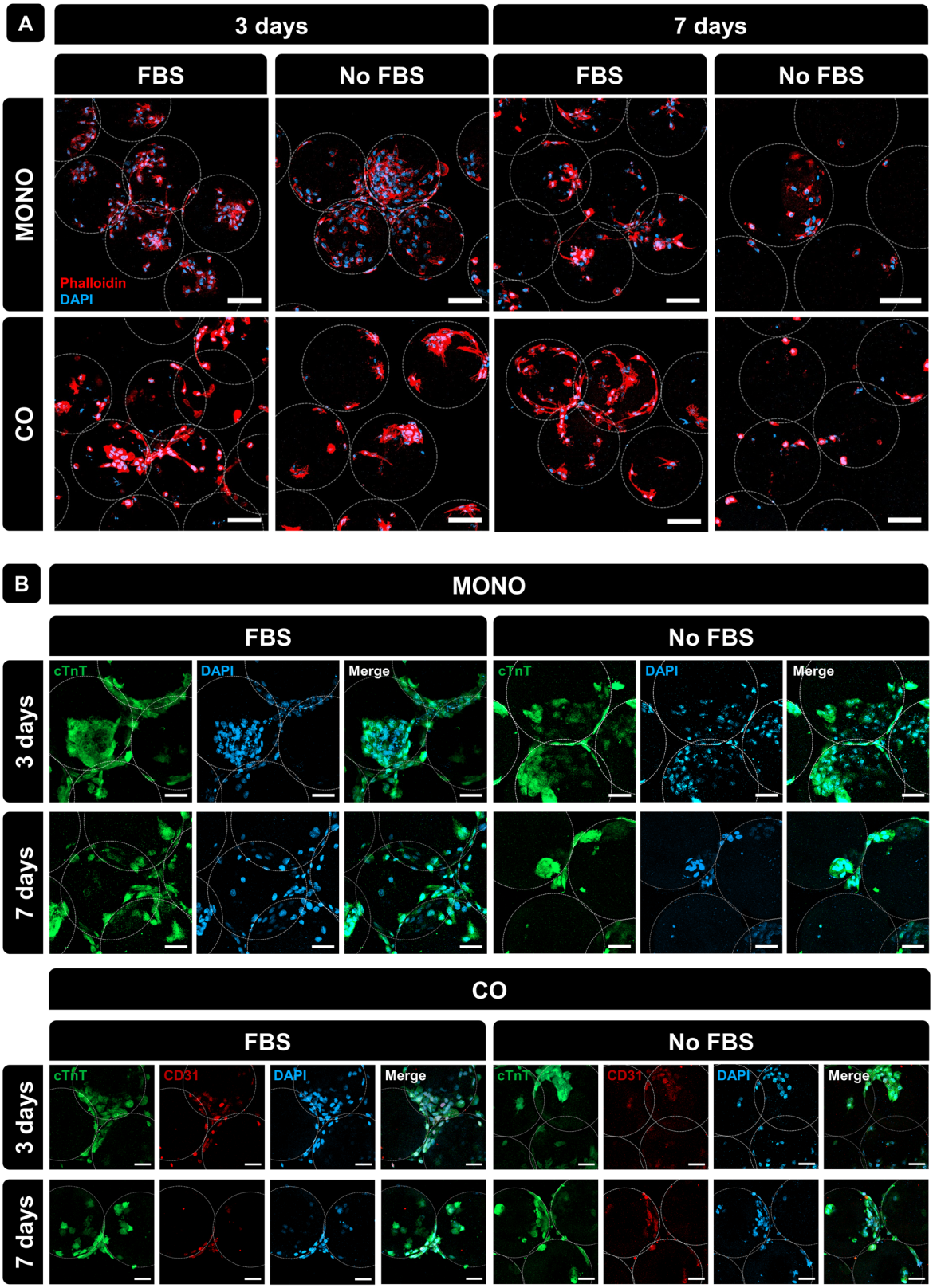

Fig. 5 Immunostaining of cells cultured in PLMA MPs. (A) Representative DAPI/phalloidin staining images of monocultured and co-cultured cells on PLMA MPs at 3 and 7 days of culture with and without FBS. (B) Representative cTnT and CD31 immunostaining images of cells monocultured and co-cultured on PLMA MPs at 3 and 7 days of culture with and without FBS. Scale bar: 100 μm.

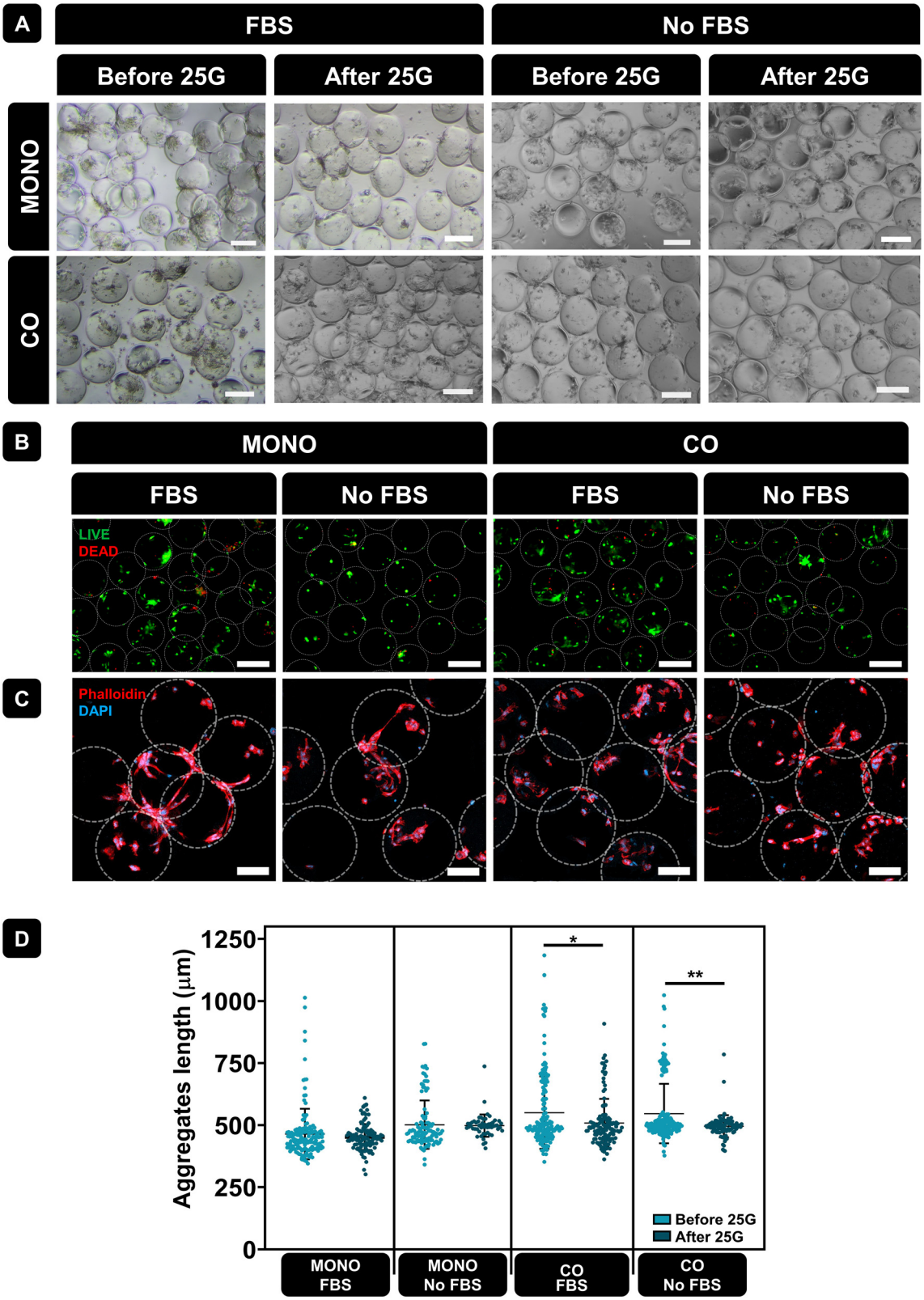

Fig. 6 PLMA MPs injectability test. (A) Representative optical microscopy images of cells in PLMA MPs at 3 days of culture before and after passing through a 25G needle. Scale bar: 200 µm. (B) Representative live/dead images of cells in PLMA MPs at 3 days of culture after passing through a 25G needle. Scale bar: 200 µm. (C) Representative DAPI/phalloidin images of cells in PLMA MPs at 3 days of culture after passing through a 25G needle. Scale bar: 100 µm. (D) PLMA MPs and cell aggregate lengths before and after 25G needle passing. Statistical analysis through one-way ANOVA combined with Tukey's multiple comparisons test showed significant differences between the analysed groups: *$p < 0.05$, **$p < 0.01$.

all conditions, meaning that the presence or absence of FBS does not affect the expression of cell surface markers. Importantly, the presence of PLMA MPs does not affect the expression of specific markers or cell phenotypes.

Microcarriers often used for tissue repair, underwent monoculture and co-culture. After 3 days of culture, PLMA microcarriers were passed through a 25G needle to assess their suitability as injectable systems for local cell delivery. Fig. 6A shows representative optical microscope images of PLMA MPs with cells pre- and post-injection, showcasing the recovery of PLMA MPs and the continued interaction of cells with the MPs. Fig. 6B shows representative live/dead images of cells in PLMA MPs after passing through the needle. Although some cell death occurred, most of the cells remained viable even under conditions without animal serum supplementation.

The morphology of cells in PLMA MPs after passing through the needle was assessed by staining F-actin filaments (phalloidin, red) and nuclei (DAPI, blue) – see Fig. 6C. Confocal images demonstrated that cells maintained their morphology, adhering to PLMA MPs, and cell–MPs aggregates remained intact. Additionally, we evaluated aggregate sizes formed between cells and PLMA MPs before and after passing through the needle. As it is shown in Fig. 6D, aggregate length is not significantly affected by needle passage under the monoculture condition. However, when under the co-culture condition, statistical analysis revealed significant differences likely attributed to larger initial aggregate sizes, which may undergo partial disintegration post-needle passage.

4. Conclusions

The development of xeno-free 3D cell culture platforms for *in situ* tissue repair systems remains a challenge in tissue engineering. Recent progress in hPL-based materials demonstrates their great potential to be used as sources for the development of platforms for cell culture in the absence of animal-derived serum supplements commonly used for this purpose. Herein, we propose a new approach regarding the use of PLMA to produce MPs to serve as anchors for cell attachment and potential injectable systems for tissue repair. PLMA MPs were able to support attachment of cardiac and endothelial cells even when no supplementation with animal-derived serum was used during cell culture time. It was also possible to conclude that such microcarriers have the ability to facilitate cell adhesion and form aggregates for potential use as injectable systems, preventing cell washout upon implantation. PLMA-based microcarriers developed in this work offer a new possibility for creating short-term injectable systems for *in situ* cell delivery and tissue repair. Importantly, they can be developed in a xeno-free environment, facilitating clinical translation processes. Besides this, it is also important to emphasize the fact that this material can have an autologous origin and thus be used to produce personalized systems for *in vitro* or *in vivo* implantation with no risk of cross-reactivity, immune reaction, or disease transmission.

Conflicts of interest

There are no conflicts to declare.

Acknowledgements

Sara C. Santos and Catarina A. Custódio acknowledge the financial support given by the Portuguese Foundation for Science and Technology (FCT) for the doctoral grant SFRH/BD/144520/2019 and individual contract 10.54499/2020.01647.CEECIND/CP1589/CT0034, respectively. The authors also acknowledge the project CICECO – Aveiro Institute of Materials, UIDB/50011/2020 (**https://doi.org/10.54499/UIDB/50011/2020**), UIDP/50011/2020 (**https://doi.org/10.54499/UIDP/50011/2020**) & LA/P/0006/2020 (**https://doi.org/10.54499/LA/P/0006/2020**), financed by national funds through the FCT/MCTES (PIDDAC). This work was also supported by the project REBORN, ERC-2019-ADG-883370 (DOI 10.3030/883370).

References

1 P. Gil-Cabrerizo, I. Scacchetti, E. Garbayo and M. J. Blanco-Prieto, *Eur. J. Pharm. Sci.*, 2023, **185**, 106439.
2 M. A. Borrelli, H. R. Turnquist and S. R. Little, *Adv. Drug Delivery Rev.*, 2021, **173**, 181–215.
3 L. Schirone, M. Forte, L. D'ambrosio, V. Valenti, D. Vecchio, S. Schiavon, G. Spinosa, G. Sarto, V. Petrozza, G. Frati and S. Sciarretta, *Cells*, 2022, **11**, 1165.
4 H. Hashimoto, E. N. Olson and R. Bassel-Duby, *Nat. Rev. Cardiol.*, 2018, **15**, 585–600.
5 L. A. Reis, L. L. Y. Chiu, N. Feric, L. Fu and M. Radisic, *J. Tissue Eng. Regener. Med.*, 2016, **10**, 11–28.
6 C. Duan, M. Yu, C. Hu, H. Xia and R. K. Kankala, *Front. Bioeng. Biotechnol.*, 2023, **11**, 1–21.
7 A. Choi, K. D. Seo, D. W. Kim, B. C. Kim and D. S. Kim, *Lab Chip*, 2017, **17**, 591–613.
8 J. P. Newsom, K. A. Payne and M. D. Krebs, *Acta Biomater.*, 2019, **88**, 32–41.
9 L. Shang, Y. Cheng and Y. Zhao, *Chem. Rev.*, 2017, **117**, 7964–8040.
10 L. Saludas, E. Garbayo, M. Mazo, B. Pelacho, G. Abizanda, O. Iglesias-Garcia, A. Raya, F. Prósper and M. J. Blanco-Prieto, *J. Pharmacol. Exp. Ther.*, 2019, **370**, 761–771.
11 E. Rosellini, N. Barbani, C. Frati, D. Madeddu, D. Massai, U. Morbiducci, L. Lazzeri, A. Falco, C. Lagrasta, A. Audenino, M. G. Cascone and F. Quaini, *J. Appl. Biomater. Funct. Mater.*, 2018, **16**, 241–251.
12 E. Garbayo, A. Ruiz-Villalba, S. C. Hernandez, L. Saludas, G. Abizanda, B. Pelacho, C. Roncal, B. Sanchez, I. Palacios, F. Prósper and M. J. Blanco-Prieto, *Acta Biomater.*, 2021, **126**, 394–407.
13 D. A. M. Feyen, R. Gaetani, J. Deddens, D. van Keulen, C. van Opbergen, M. Poldervaart, J. Alblas, S. Chamuleau,

L. W. van Laake, P. A. Doevendans and J. P. G. Sluijter, *Adv. Healthcare Mater.*, 2016, **5**, 1071–1079.
14 X. Wang, A. Ansari, V. Pierre, K. Young, C. R. Kothapalli, H. A. von Recum and S. E. Senyo, *Adv. Healthcare Mater.*, 2022, **11**, 2102265.
15 J. P. Karam, C. Muscari, L. Sindji, G. Bastiat, F. Bonafè, M. C. Venier-Julienne and N. C. Montero-Menei, *J. Controlled Release*, 2014, **192**, 82–94.
16 E. Garbayo, J. J. Gavira, M. G. De Yebenes, B. Pelacho, G. Abizanda, H. Lana, M. J. Blanco-Prieto and F. Prosper, *Sci. Rep.*, 2016, **6**, 1–12.
17 J. Tang, D. Shen, T. G. Caranasos, Z. Wang, A. C. Vandergriff, T. A. Allen, M. T. Hensley, P. U. Dinh, J. Cores, T. S. Li, J. Zhang, Q. Kan and K. Cheng, *Nat. Commun.*, 2017, **8**, 1–9.
18 A. Hameed, L. B. Gallagher, E. Dolan, J. O'Sullivan, E. Ruiz-Hernandez, G. P. Duffy and H. Kelly, *J. Microencapsulation*, 2019, **36**, 267–277.
19 J. Feng, Y. Wu, W. Chen, J. Li, X. Wang, Y. Chen, Y. Yu, Z. Shen and Y. Zhang, *J. Mater. Chem. B*, 2020, **8**, 308–315.
20 M. Shin, K. H. Song, J. C. Burrell, D. K. Cullen and J. A. Burdick, *Adv. Sci.*, 2019, **6**, 1–8.
21 A. R. Anderson and T. Segura, *J. Visualized Exp.*, 2022, (188), e64554.
22 S. C. Santos, Ó. E. Sigurjonsson, C. A. Custódio and J. F. Mano, *Tissue Eng., Part B*, 2018, **24**, 454–462.
23 T. Burnouf, M. L. Chou, D. J. Lundy, E. Y. Chuang, C. L. Tseng and H. Goubran, *J. Biomed. Sci.*, 2023, **30**, 1–34.
24 S. C. Santos, C. A. Custódio and J. F. Mano, *Adv. Healthcare Mater.*, 2018, **7**, 1–12.
25 M. T. Tavares, S. C. Santos, C. A. Custódio, J. P. S. Farinha, C. Baleizão and J. F. Mano, *Mater. Today Bio*, 2021, **9**, 100096.
26 C. F. Monteiro, S. C. Santos, C. A. Custódio and J. F. Mano, *Adv. Sci.*, 2020, **7**, 1902398.
27 C. F. Monteiro, C. A. Custódio and J. F. Mano, *Acta Biomater.*, 2021, **134**, 204–214.
28 S. C. Santos, C. A. Custódio and J. F. Mano, *Adv. Healthcare Mater.*, 2022, **11**, 2102383.
29 C. Shao, J. Chi, L. Shang, Q. Fan and F. Ye, *Acta Biomater.*, 2022, **138**, 21–33.
30 J. M. Duarte Rojas, L. M. Restrepo Múnera and S. Estrada Mira, *Biomedicines*, 2024, **12**, 140.
31 M. Cañas-Arboleda, K. Beltrán, C. Medina, B. Camacho and G. Salguero, *Int. J. Mol. Sci.*, 2020, **21**, 6284.
32 K. Kalra, J. Eberhard, N. Farbehi, J. J. Chong and M. Xaymardan, *Front. Cell Dev. Biol.*, 2021, **9**, 669188.
33 J. H. Lee, P. Parthiban, G. Z. Jin, J. C. Knowles and H. W. Kim, *Prog. Mater. Sci.*, 2021, **117**, 100732.
34 I. Prudovsky, *Cells*, 2021, **10**, 1830.